Int. J. Heat Mass Transfer. Vol. 35, No. 10, pp. 2327–2334, 1992
Printed in Great Britain

0017–9310/92 $5.00 + 0.00

Natural convection heat transfer between a uniformly heated cylindrical element and its rectangular enclosure

NASRINE K. GHADDAR†

American University of Beirut, Faculty of Engineering and Architecture, Mechanical Engineering, Beirut, Lebanon

(*Received* 30 *January* 1991 *and in final form* 11 *November* 1991)

Abstract—A numerical study of natural convection heat transfer from a uniformly heated horizontal cylinder placed in a large air-filled rectangular enclosure, is performed using a spectral element method. The enclosure walls are isothermal and the flow is assumed laminar and two-dimensional. Dynamics of the flow and the thermal behavior is studied at various heat fluxes applied to the cylinder. It is found that the mean Nusselt number, Nu_a, varies with Rayleigh number, Ra_a, according to a general correlation of the form $Nu_a = C_1(Ra_a)^{C_2}$, where C_1 and C_2 are empirical constants that depend on the chosen scale length a. The resulting correlation constants C_2 are similar to previously published correlation constants based on experimental data. The highest heat transfer rates out of the enclosure occur at the top wall. For all examined heat fluxes, the maximum air velocity is at a distance of about nine cylinder diameters along the vertical centerline above the heated cylinder.

INTRODUCTION

NATURAL convection heat transfer in enclosures has been the subject of numerous investigations in recent years. There is a growing demand for a better understanding of this phenomenon in areas like nuclear design, electronic packaging, passive cooling space heating, and geophysical systems. Comparatively quite a bit of work is being done on internal free convective heat transfer from bodies within an enclosure. The most extensive work in this area has been concerned with isothermal horizontal cylinders or spheres placed symmetrically within horizontal cylindrical or spherical enclosures, e.g. see the work of Sun and Zhang [1], Roy and Sengupta [2], Projahn *et al.* [3] and Powe and Warrington [4]. Experimental studies of natural convection heat transfer between concentrically mounted bodies (spheres, cylinders and cubes) and their non-spherical (cubical) enclosures were reported by Warrington and Powe [5] at moderate Rayleigh numbers and by Warrington *et al.* [6] at low Rayleigh numbers. In both studies some correlations between Nusselt number and Rayleigh number were developed and the effect of enclosure shape was seen to be small so long as the appropriate length scale was employed. Numerical results on natural convection heat transfer from a prismatic cylinder in a square enclosure were reported by Oosthuizen and Paul [7]. Their study showed that the inner body shape (aspect ratio: height/width) affected the heat transfer rates from the isothermal hot body such that at low aspect ratios, $(Nu/Ra)^{1/4}$ was approximately constant while at large aspect ratios, $(Nu/Ra)^{1/2}$ was approximately constant. They also showed that increasing the cavity size had increased the convective motions and the mean Nusselt number had approached a constant value of infinite environment.

The intent of the present paper is to numerically study the details of natural convection heat transfer in air at atmospheric pressure from a uniformly heated inner cylinder to a rectangular isothermal enclosure. Numerical simulations of the problem are done at various heat transfer rates from the cylinder using the spectral element method developed by Patera [8], Korzsak and Patera [9] and Ghaddar *et al.* [10]. Velocity and temperature fields are obtained and the effect of increasing the heat transfer rates is studied. Correlation equations are obtained and their form and trend are compared with reported experimental correlations.

PROBLEM FORMULATION AND NUMERICAL PROCEDURE

The physical situation and coordinate system of the problem are illustrated systematically in Fig. 1, where a cylindrical element of diameter $d = 0.63$ cm is placed at a height l from the bottom wall of an air-filled ($Pr = 0.72$) rectangular enclosure of height H and width W. The geometry dimensional ratios are: $H/D = 40$, $W/d = 15$, and $l/d = 10$. A constant heat flux is applied to the surface of the cylinder, while the enclosure wall temperature is assumed constant. The heat transfer in the air cavity is modelled as a two-

† Address for correspondence: American University of Beirut, Faculty of Engineering and Architecture, Department of Mechanical Engineering, 850 Third Avenue, 18th Floor, New York, NY 10022, U.S.A.

NOMENCLATURE

a	any characteristic length
b	distance travelled by the boundary layer on the cylinder
C_1, C_2	empirically determined constants
C_p	specific heat at constant pressure for air ($=0.2416$ cal g^{-1} K^{-1})
d	cylinder diameter
g	gravitational acceleration, 981 cm s^{-2}
h	average heat transfer coefficient
H	enclosure height
k, k_{cond}	thermal conductivity of air ($=0.62476\times10^{-4}$ cal cm^{-1} s^{-1} K^{-1})
k_{eff}	effective thermal conductivity
l	height at which the cylinder is placed in the enclosure
L	hypothetical gap width
N	order of grid spectral resolution
Nu_a	Nusselt number, ha/k
Pr	Prandtl number, $C_p\rho v/k$
q	heat flux at the cylinder surface
Q	ratio of K_{eff}/k_{cond}
r_i	cylinder radius
Ra_L	Rayleigh number, $Ra_L = g\beta C_p(T_m - T_w)L^3/\nu\alpha$
Ra^*	modified Rayleigh number ($=Ra(L/r_i)$)
t	time
T	local temperature [K]
T_m	mean temperature of the cylinder
ΔT_c	temperature difference $T_{max} - T_{min}$ on cylinder
T_w	enclosure wall temperature [K]
u	horizontal component of the velocity
v	vertical component of the velocity
$v_{up,max}$	maximum upward speed in the enclosure
W	enclosure width.

Greek symbols

β	thermal expansion coefficient of air ($=0.2645$ K^{-1})
θ	angular position on cylinder surface
ν	kinematic viscosity of air ($=0.275$ cm^2 s^{-1})
ρ	density of air ($=0.9403\times10^{-3}$ g cm^{-3}).

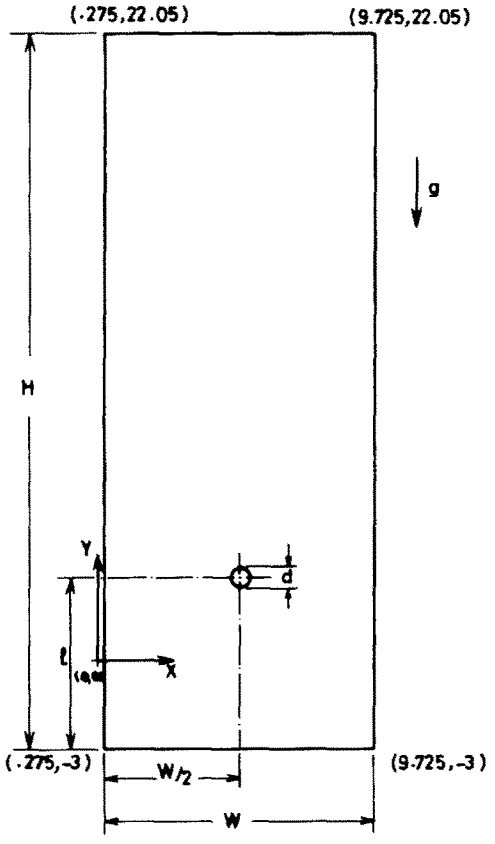

FIG. 1. Physical situation and coordinate system (dimensions are all in cm).

dimensional, laminar natural convection flow. The governing equations for the present problem, neglecting viscous dissipation and compressibility effects, are the Navier–Stokes (1), continuity (2) and energy (3) equations given by

$$\frac{\partial u}{\partial t}+u\frac{\partial u}{\partial x}+v\frac{\partial u}{\partial y}=-\frac{1}{\rho}\frac{\partial p}{\partial x}+\nu\left(\frac{\partial^2 u}{\partial x^2}+\frac{\partial^2 v}{\partial y^2}\right) \quad (1a)$$

$$\frac{\partial v}{\partial t}+u\frac{\partial v}{\partial x}+v\frac{\partial v}{\partial y}=-\frac{1}{\rho}\frac{\partial p}{\partial x}+\nu\left(\frac{\partial^2 v}{\partial x^2}+\frac{\partial^2 v}{\partial y^2}\right)+\beta g(T-T_w) \quad (1b)$$

$$\frac{\partial u}{\partial x}+\frac{\partial v}{\partial y}=0 \quad (2)$$

$$\frac{\partial T}{\partial t}+u\frac{\partial T}{\partial x}+v\frac{\partial T}{\partial y}=\frac{k}{\rho C_p}\left(\frac{\partial^2 T}{\partial x^2}+\frac{\partial^2 T}{\partial y^2}\right). \quad (3)$$

The hydrodynamic boundary conditions are the no-slip condition of $u=v=0$ at the solid walls. The thermal boundary conditions are the uniform enclosure wall temperature at $T_w = 288$ K and the constant heat flux $q = k\,\partial T/\partial n$ at the cylinder wall, where $\partial/\partial n$ refers to differentiation along the outward normal from the surface. A positive flux, q, corresponds to heat flux into the enclosure. The initial conditions to the problem are taken as zero velocity (no motion) and a uniform air temperature of $T(x, y, t=0) = 288$ K.

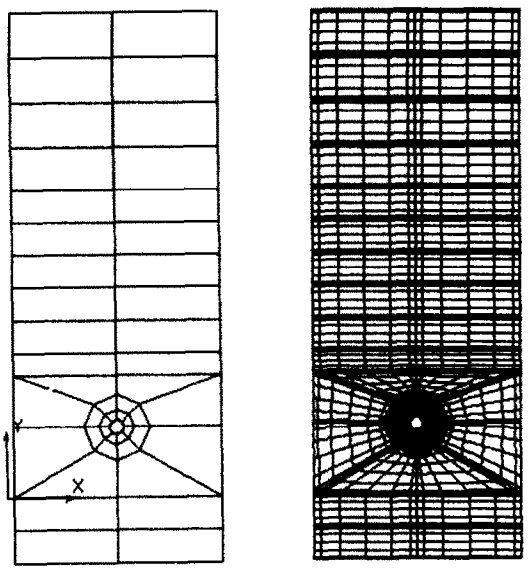

FIG. 2. The computational domain divided into 48 macro-elements with a spectral resolution of 7×7 in each element.

The steady-state solution to the system of coupled equations (1)–(3) together with the boundary conditions are obtained numerically via a transient direct approach along with the spectral element method. The spectral element method combines the geometric flexibility of finite element methods with the high-order exponential convergence rates, good resolution properties and minimal dispersion errors of the global spectral methods [1]. In the present study the spectral element Nekton computer code has been used.

The code was developed by Korszak and Patera [9], and modified by Ghaddar *et al.* [12] and Karniadakis *et al.* [13].

The grid system used, as shown in Fig. 2, is composed of 48 macro elements with $N \times N$ ($N = 7$) local spectral resolution, where N represents the order of the Lagrangian interpolants internal to the element in each direction. The element decomposition allows for a very flexible resolution and point distribution in the computational domain, where more elements are distributed near the heated cylinder. The dependent variables (u, v, p, T) and the independent variables (geometry) are all represented by the high order elemental Lagrangian interpolants through Chebyshev (cosine) collocation points. The Chebyshev nodes automatically cluster near boundaries of the elements. This is used to the advantage of resolving thin hydrodynamics and thermal boundary layers in the region around the cylinder, where the highest gradients of temperature and velocity are expected to occur. The non-linear convective terms and the buoyant terms are treated by explicit collocation, while the implicit pressure and diffusive terms are handled using variational projection operators.

In regard to time stepping method associated with the spectral discretization, a semi-implicit fractional step method is used [14]. The convective terms and the buoyant coupling term in the governing equations are treated by explicit collocation with a third-order Adams–Bashforth scheme, which decouples the momentum and energy equations. This is followed by a split pressure step that uncouples continuity and pressure equations by using an inviscid pressure boundary condition.

The viscous and conduction terms are treated implicitly using the Crank–Nicolson scheme as a final step. The full boundary conditions of velocity and temperature are imposed on the viscous and conduction steps for both momentum and energy equation, respectively. The method has a temporal accuracy of order Δt^2 for the velocities and a splitting error for the pressure of order $\mu \Delta t$.

INPUT PARAMETERS

Simulations are done for the air-filled enclosure problem for six different values of heat flux q on the cylindrical element surface, ranging from $q = 0.115 \times 10^{-2}$ to $q = 0.3047 \times 10^{-1}$ cal cm^{-2} s^{-1}, as listed in Table 1.

Most of the calculations are done using the grid system shown in Fig. 2, which has 1848 nodes, but at high fluxes the resolution N is increased from 7 to 9. The time step size Δt for the numerical solution is governed by the Courant number stability condition of $c = (\Delta t V_{max}/\Delta s) < 0.7$, where Δs is the minimum grid size in either x or y direction. In the simulations, the minimum grid size was of the order 10^{-3} cm near the cylinder while the time step size Δt was of the order 10^{-4} s. The calculations were performed on a VAX8820 at Kuwait University computing facility. An average run took about 250 h of CPU time resulting from the restricted small size of the time step.

The solutions were checked for being convergent in both time-step and spatial degrees of freedom. The convergence criterion was set relative to the change in temperature. Convergence was achieved when the maximum absolute change in temperature was less than 10^{-3}. At this level, relative changes in velocities were about 0.01%.

Another test on the numerical solution reliability was done by performing an energy balance to verify that the total heat transferred through the enclosure walls was actually equal to the total heat input dissipated from the cylinder surface. For example in run

Table 1. List of simulations

Run	q (cal cm^{-2} s^{-1})	Grid spectral resolution N per element
1	0.1150×10^{-2}	7
2	0.2300×10^{-2}	8
3	0.4200×10^{-2}	8
4	0.6900×10^{-2}	9
5	0.1550×10^{-1}	9
6	0.3047×10^{-1}	9

(3), the heat fluxes integrated over the top, side and bottom walls of the enclosure were -0.00387, -0.00543, $+0.000875$ cal cm^{-1} s^{-1}, respectively. Note that the heat flux direction at the bottom wall was into the enclosure. The total heat input from the cylinder was $+0.00831$ cal cm^{-1} s^{-1} with an error difference in the balance of 1.4%.

In the following, the physical aspects of the flow and temperature fields are presented for sample runs. Then the overall heat transfer results are discussed in an appropriate form.

RESULTS AND DISCUSSION

Flow patterns: velocity and temperature fields

Typical flow patterns and isotherms in the enclosure domain are presented, by means of velocity distributions and contour plots of streamlines and isotherms, for the conditions of run 2 and run 5 representing cases of low and high heat flux.

Figure 3 illustrates the streamline patterns for the selected runs. A layer of hot fluid moves up along the cylinder at high speed to reach the enclosure top and comes down along the cool walls of the enclosure at reduced speeds completing a recirculation flow pattern. Three regions of almost stagnant air appear in the streamline plots. One such region is the lower zone near the bottom enclosure wall where the flow below the cylinder is driven in the upward direction leaving that lower region undisturbed. The two other stagnation regions, around which the air is moving, are located symmetrically away from the vertical centerline of the enclosure with their centers in the mid-upper region. The variation of the upward v-velocity of air along the vertical symmetry-line is plotted from the cylinder surface up to the top wall as shown in Fig. 4. A general trend is observed in both of the selected runs. The upward velocity reaches a first maximum at some fixed height from the cylinder and then a second local maximum of v_{up} appears at some distance close to the upper wall. This second increase in v_{up} is due to the relative increase in the driving thermal gradient forces near the upper isothermal stagnation wall.

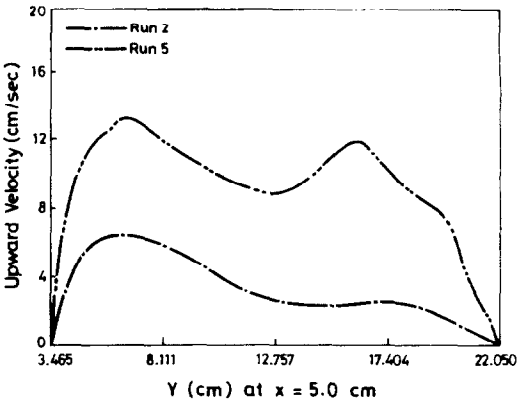

FIG. 4. The variation of the upward v-velocity of air along the vertical symmetry line from the cylinder top to the upper enclosure wall for runs 2 and 5.

The isotherms shown in Fig. 5 are uniformly incremented. The temperature distributions indicate

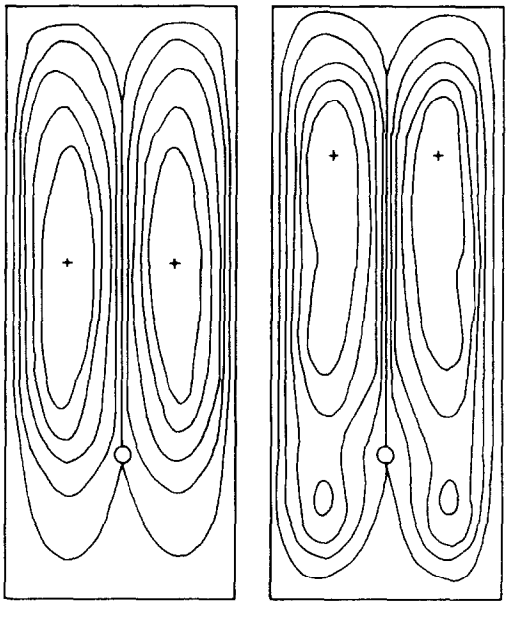

FIG. 3. Streamline patterns for runs 2 and 5 where the flow rates of the recirculating regions are 7 cm^2 s^{-1} and 17 cm^2 s^{-1} for run 2 and run 5, respectively.

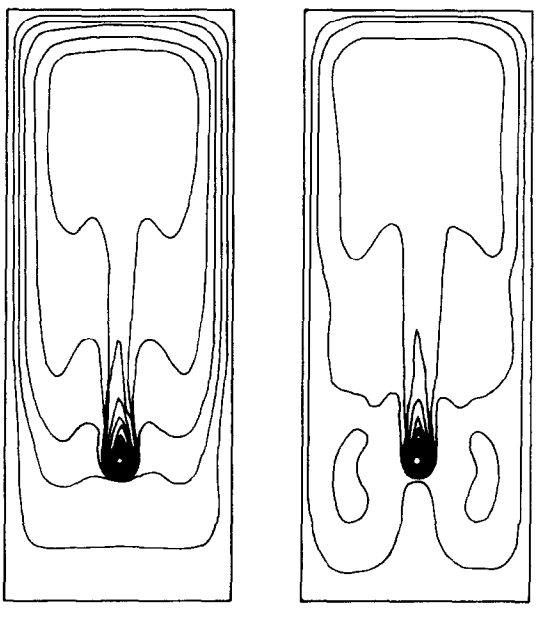

FIG. 5. Twenty equally spaced isotherm plots for runs 2 and 5. The isotherm range ($T_{max} - T_w$) is 15.31 K for run 2 and 81.3 for run 5. The thermal plume is clearly seen for both runs.

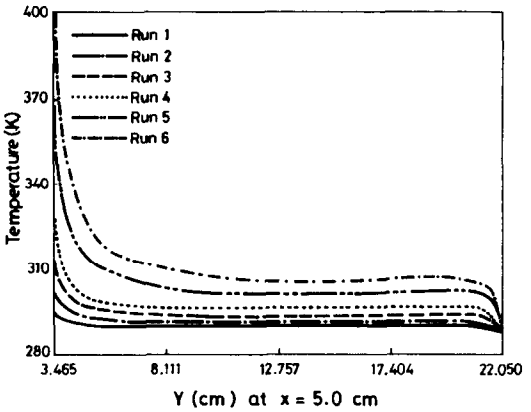

FIG. 6. Temperature distributions on the vertical symmetry line from the cylinder top surface to the top wall at various heat fluxes.

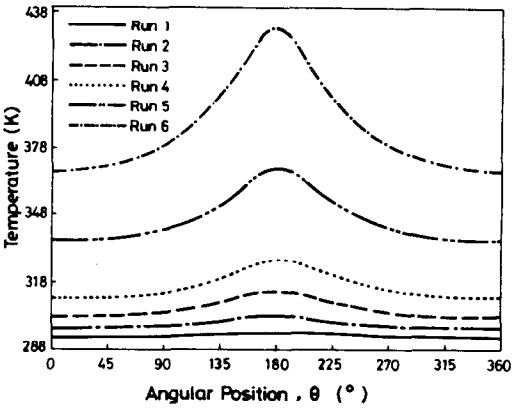

FIG. 7. The temperature distribution around the cylinder surface vs the angular position (θ) where $\theta = 0$ at the cylinder lowest point.

the presence of a thermal plume above the cylinder where the boundary layer separates. The temperature profile near the bottom indicates the dominance of conduction heat transfer in that cold, stagnant region.

A large region above the cylinder, in the middle and upper part of the enclosure, is almost at a constant temperature. The rising hot air diffuses the heat by conduction to the surrounding area while reaching the far top wall. The steepest drop in temperature occurs near the cylinder surface as can be seen in Fig. 6, which shows the temperature distribution along the vertical centerline for both the representative cases. The maximum temperature in the domain occurs at the top of the hot cylindrical surface, while an almost constant temperature distribution pertains in the middle region of the enclosure. Note that the thermal boundary layer thickness at the cylinder surface is thinner at the high heat flux case compared with the low flux case. A relatively steep drop in temperature occurs again near the top wall consistent with the observation of increased air flow in that region (see Fig. 6). Actually the maximum heat flux loss through the enclosure walls occurs at the middle of the top wall at $x = 5.0$ cm, $y = 22.05$ cm.

The temperature distribution around the cylinder surface is plotted against angular position (θ) for the selected cases as shown in Fig. 7. The temperature distribution is symmetric about the vertical centerline and larger variations of temperature occur near the cylinder top (hotter region) compared with the lower half of the cylinder surface (colder region). The higher temperature on the upper surface of the cylinder would tend to augment the driving potential for convective motion above the cylinder thus resulting in higher Nusselt numbers than if the cylinder is made isothermal [5].

Thermal patterns of free convection solution are also compared with the pure conduction isotherms for the same geometry and the same thermal boundary conditions. Figure 8 shows isotherm patterns of the conduction problem of run 2. Higher gradients of temperature are observed near the cylinder, while the upper region is almost isothermal. The conduction solutions obtained can account for the geometric effect on convective heat transfer.

Overall momentum and heat transfer results

To overlook all the physical aspects of increased heat flux, from the heating element to the air-filled enclosure, a parametric study is performed.

First, we show in Fig. 9 the variation of the maximum upward velocity $v_{up,max}$ with imposed heat flux. There is almost a linear increase of $v_{up,max}$ with increased heat flux. The interesting result here is that the maximum upward speed occurs at an almost fixed distance y_v above the cylinder top surface. The distance y_v is about nine cylinder diameters and rep-

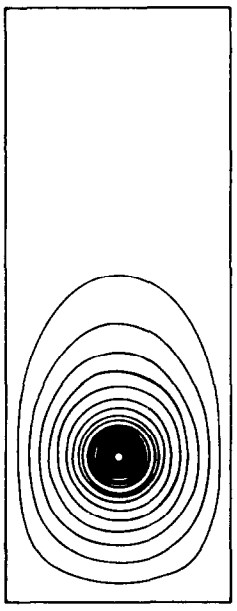

FIG. 8. Twenty equally spaced isotherm range ($T_{max} - T_w$) is 33.7 K.

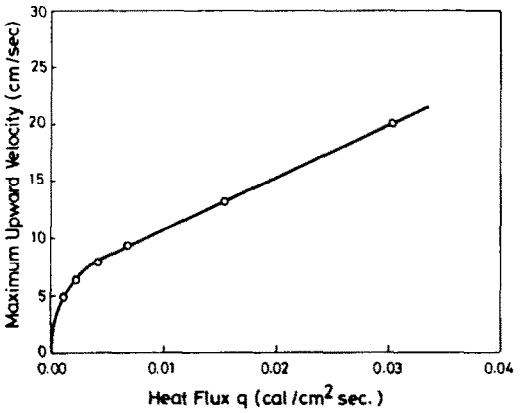

FIG. 9. Variation of the maximum upward velocity with the imposed heat flux.

resents 30% of the total distance from the cylinder to the top wall. The similarity in the flow patterns and velocity distributions is expected, since only the heat flux is varied for the given fixed geometry.

The difference between maximum and minimum temperatures on the cylinder surface, $\Delta T_c = (T_{max} - T_{min})$ is plotted against the heat flux in Fig. 10. A rapid increase in the temperature difference is observed at lower values of the heat flux, while a gradual increase is observed at high fluxes. This may be due to boundary layer separation effects at higher heat fluxes (higher Rayleigh numbers).

One of our primary objectives is also to find a relationship between the dimensionless quantities of Nusselt number, Rayleigh number and an appropriate geometric parameter. The mean Nusselt number and Rayleigh number are defined by

$$Nu_L = qL/K(T_m - T_w) \tag{4}$$

$$Ra_L = g\beta C_p(T_m - T_w)L^3/\nu\alpha. \tag{5}$$

The length term L, is a hypothetical gap width between the inner body and the enclosure wall, L is defined as the distance from an imaginary outer cylindrical enclosure whose volume is equal to the

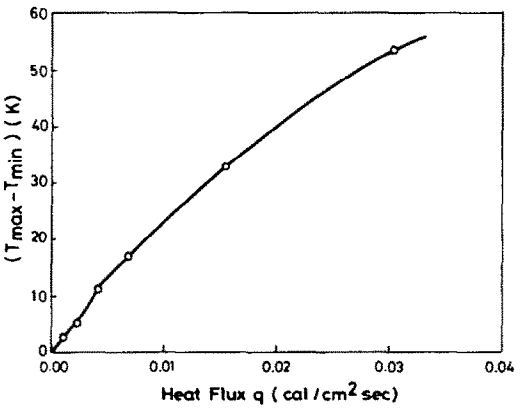

FIG. 10. A plot of temperature difference $(T_{max} - T_{min})$ on the cylinder surface vs the heat flux q.

rectangular enclosure. Alternatively, the length scale can also be taken as the length scale, b, for free convection in infinite atmosphere, which is the distance travelled by the boundary layer on the inner body assuming no boundary layer separation. This distance, which has been first proposed by Lienhard [15], is taken as $b = d\pi/2$. In our problem the heat transfer results are correlated as well by an infinite atmosphere gap width ($L = 48b$).

Many previous analyses [3, 4, 7] of the enclosure heat transfer data have shown that correlations of the form

$$Nu_L = C_1\, Ra_L^{C_2} \tag{6}$$

$$Nu_b = C_1\, Ra_b^{C_2} \tag{7}$$

could correlate extremely well concentric and eccentric spherical and cylindrical data and cubes to a spherical or cubical enclosure. Correlations of heat transfer data for air as the test fluid reported by Warrington and Powe [5] are given by $Nu_L = 0.173 Ra_L^{*0.299}$ and $Nu_b = 0.833 Ra_b^{0.237}$, where $Ra_L^* = Ra_L(L/r_i)$ is the modified Rayleigh number. Other correlations have considered [5, 6, 16, 17] the ratio of an effective convection conductivity to that of conduction ($Q = K_{eff}/K_{cond}$) and have correlated it to the modified Rayleigh number, Ra_L^*, in the form

$$Q = (T_m - T_w)_{cond}/(T_m - T_w)_{conv} = C_1\, Ra_L^{*C_2}. \tag{8}$$

The experimental correlation for air data reported by Warrington and Powe [5] has $C_1 = 0.479$ and $C_2 = 0.171$. For our problem the parameter Q may not be the superior correlating parameter since the enclosure size is large compared with the size of the inner body. The equations (6)–(8) are used to correlate the heat transfer data for our case of uniform heat flux (non-isothermal) inner surface. The empirical constants are determined using a standard least-squares curve fitting technique. The heat transfer correlations obtained from the numerical results are given by

$$Nu_L = 1.81 Ra_L^{*0.207} \tag{9}$$

with an average deviation of 7.4%,

$$Nu_b = 0.604 Ra_b^{0.2083} \tag{10}$$

with an average deviation of 19.9%, and

$$Q = 0.041 Ra_L^{*0.228} \tag{11}$$

with an average standard deviation of 22%.

In Fig. 11, the heat transfer correlation of Nu_L and Ra_L^* is plotted for both the numerical results and the predicted values of Warrington and Powe correlation for air [5]. The numerical values in this case predict slightly higher Nusselt number than the experimental correlation for $Ra_L^* < 10^9$. The discrepancy, even though small, can be related to the difference in conditions upon which experimental correlations are based, where three-dimensional effects may be present and an isothermal inner surface is set. The effect of

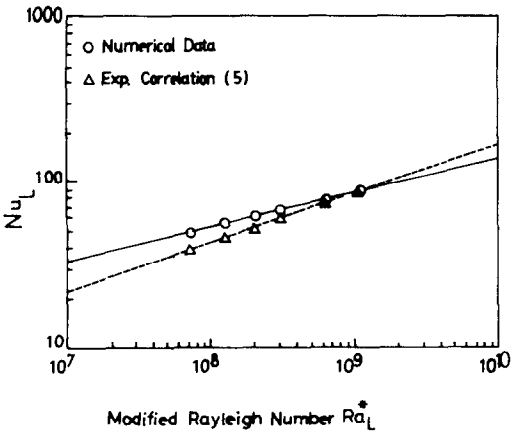

FIG. 11. Heat transfer correlation of Nu_L vs Ra_L^*.

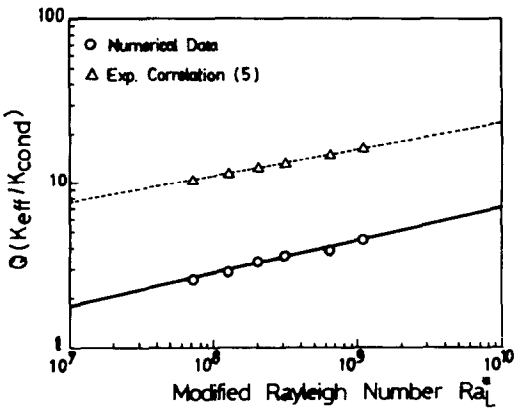

FIG. 13. Heat transfer correlation of convection to conduction ratio Q vs the modified Rayleigh number Ra_L^*.

the non-isothermal condition on the inner element have been verified to be well represented by the isothermal reported experimental correlation of Warrington and Powe [5]. At lower Rayleigh number, this effect in general would, however, tend to augment the driving potential for heat transfer resulting in larger Nusselt number than the isothermal case. This can be clearly seen from Fig. 11, where the isothermal correlation fits better with our numerical results at high Rayleigh number.

Figure 12 shows the numerically obtained correlation of Nu_b and Ra_b with the predicted values of Nu_b from the experimental correlation of Warrington and Powe [5]. The experimental correlation based on length scale b gives higher estimates of Nusselt number than length b, which usually works well for infinite atmosphere, is not the proper parameter in our model problem.

Figure 13 shows the variation of convection to conduction ratio Q vs the modified Rayleigh number for both the numerical correlation (11) and the experimentally based one of Warrington and Powe [5]. The numerical model gives much lower values of Q than the experimental predictions. The most deviation between experimentally and numerically based correlations which occurred was the $Q - Ra_L^*$ correlation. This is expected since the experimental correlation is valid only for small values of L/r_i. As L/r_i is decreased Q would become the superior dependent correlating parameter [5, 6].

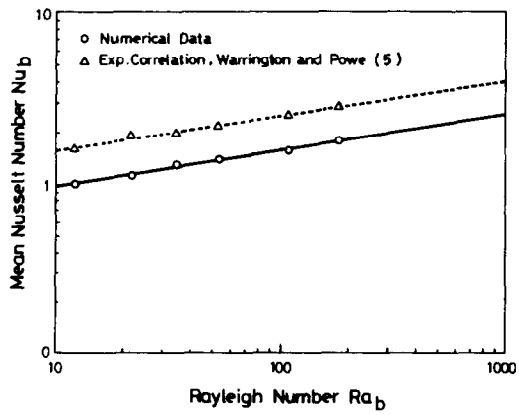

FIG. 12. Heat transfer correlation of Nu_b vs Ra_b.

CONCLUSIONS

The present numerical study of natural convection has brought out the prominent physical features of convective motions and heat transfer from a uniformly heated cylindrical source within an air-filled isothermal enclosure. The temperature and velocity profiles have displayed remarkable similarity at different Rayleigh numbers and have been consistent with the behaviour observed by previous investigators.

Correlations for heat transfer have been obtained relating Nusselt number to Rayleigh number. The best correlation for heat transfer for our problem is the one based on the hypothetical gap width, L. The correlation based on conduction solutions is the one that had the most deviation from experimentally-based correlation.

Acknowledgement—I would like to thank Mr Rami Mansour for his assistance in performing the computer simulations. I also would like to acknowledge the support of the Scientific Computing Department at Kuwait University.

REFERENCES

1. Renqia Sun and Xing Zhang, An experimental study of the natural convection within the horizontal cylindric annular enclosures, *Proc. 8th Int. Heat Transfer Conf.*, Vol. 4, pp. 1569–1576. ASME (1986).
2. S. K. Roy and S. Sengupta, A numerical study of natural convection heat transfer in a vertically eccentric spherical annulus, *Int. Commun. Heat Mass Transfer* **15**, 615–626 (1988).
3. U. Projahn, H. Reiger and H. Beer, Numerical analysis of laminar natural convection between concentric and eccentric cylinders, *Numer. Heat Transfer* **4**, 131–146 (1981).

4. R. E. Powe and R. O. Warrington, Natural convection heat transfer between bodies and their spherical enclosure, *J. Heat Transfer* **105,** 440–446 (1983).
5. R. O. Warrington and R. E. Powe, The transfer of heat between their bodies and their enclosures, *Int. J. Heat Mass Transfer* **28,** 319–330 (1985).
6. R. O. Warrington, P. K. Brown and R. E. Powe, Natural convection heat transfer within enclosures at reduced pressures, *Proc. 8th Int. Heat Transfer Conf.*, Vol. 4, pp. 1483–1488. ASME (1986).
7. P. H. Oosthuizen and J. T. Paul, Finite element study of natural convection heat transfer from a prismatic cylinder in an enclosure, *Numer. Meth. Heat Transfer*, HTD Vol. 62, pp. 13–21. ASME (1987).
8. A. T. Patera, A spectral element method for fluid dynamics: laminar flow in a channel expansion, *J. Comput. Phys.* **54,** 468–488 (1984).
9. K. Z. Korzsak and A. T. Patera, An isoparametric spectral element method for solution of the Navier–Stokes equations in complex geometry, *J. Comput. Phys.* **62,** 361–379 (1986).
10. N. K. Ghaddar, G. E. Karniadakis and A. T. Patera, A conservative isoparametric spectral element method for forced convection: application to fully-developed flow in periodic geometries, *Numer. Heat Transfer* **9,** 227–300 (1986).
11. D. O. Gottlieb and S. A. Orszag, *Numerical Analysis of Spectral Methods*. SIAM, Philadelphia (1977).
12. N. K. Ghaddar, K. Z. Korszak, B. B. Mikic and A. T. Patera, Numerical investigation of incompressible flow in grooved channels, Part 1. Stability and self-sustained oscillations, *J. Fluid Mech.* **163,** 99–127 (1986).
13. G. E. Karniadakis, E. T. Bullister and A. T. Patera, A spectral element method for solution of two and three-dimensional, time-dependent incompressible Navier Stokes equations, *Proc. Int. Symposium on Finite Element Methods for Nonlinear Problems*. Springer, Berlin (1985).
14. S. A. Orszag and L. C. Kells, Transition to turbulence in plane Poiseuille and plane Couette flows, *J. Fluid Mech.* **96,** 159–178 (1980).
15. J. Lienhard, The commonality of equations for natural convection from immersed bodies, *Int. J. Heat Mass Transfer* **16,** 2121–2123 (1973).
16. J. A. Scanlan, E. H. Bishop and R. E. Powe, Natural convection heat transfer between concentric spheres, *Int. J. Heat Mass Transfer* **13,** 1857–1872 (1970).
17. C. T. McCoy, R. E. Powe, E. H. Bishop, N. Weber and J. Scanlan, Free convection between a vertical cylinder and a spherical enclosure, *Proc. Fifth Int. Heat Transfer Conf.*, Tokyo, Vol. 3, Paper No. NC3.5, pp. 105–109 (1974).

CONVECTION THERMIQUE NATURELLE ENTRE UN ELEMENT CYLINDRIQUE CHAUD ET SON ENCEINTE RECTANGULAIRE

Résumé—Une étude numérique de convection thermique naturelle pour un cylindre horizontal chauffé uniformément et placé dans une grande enceinte rectangulaire emplie d'air, est conduite en utilisant une méthode à élément spectrale. Les parois de l'enceinte sont isothermes et l'écoulement est supposé laminaire et bidimensionnel. La dynamique de l'écoulement et le comportement thermique sont étudiés pour différents flux thermiques appliqués au cylindre. On trouve que le nombre de Nusselt moyen $Nu_a = C_1(Ra_a)^{C_2}$ où C_1 et C_2 sont des constantes empiriques qui dépendent de l'échelle de longueur choisie a. Les constantes C_2 sont semblables à celles déjà publiées et basées sur l'expérience. Les plus grands flux thermiques hors de l'enceinte sont localisés sur la paroi supérieure. Pour tous les cas examinés, la vitesse d'air maximale est obtenue à une distance de neuf diamètres de cylindre environ, sur la ligne des centres verticales au dessus du cylindre.

WÄRMEÜBERGANG DURCH NATÜRLICHE KONVEKTION ZWISCHEN EINEM GLEICHFÖRMIG BEHEIZTEN ZYLINDER UND SEINER RECHTECKIGEN UMSCHLIESSUNG

Zusammenfassung—Der Wärmeübergang durch natürliche Konvektion zwischen einem gleichförmig beheizten horizontalen Zylinder, der sich in einem großen, luftgefüllten rechteckigen Hohlraum befindet, wird numerisch mit Hilfe eines Spektral-Element-Verfahrens untersucht. Die Wände des Hohlraums sind isotherm, und die Strömung wird als laminar und zweidimensional angenommen. Das instationäre Verhalten der Strömung und der Temperaturen wird bei unterschiedlichen Wärmestromdichten am Zylinder untersucht. Dabei ergibt sich, daß die mittlere Nusselt-Zahl Nu_a sich mit Rayleigh-Zahl Ra_a entsprechend der allgemeinen Korrelation $Nu_a = C_1(Ra_a)^{C_2}$ ändert, wobei C_1 und C_2 empirische Konstanten sind, die ihrerseits von der Wahl der charakteristischen Abmessung a abhängen. Es ergeben sich Korrelationskonstanten C_2, die ganz ähnlich sind wie die Konstanten aus früheren Versuchsreihen. Die höchsten Wärmeübergangskoeffizienten ergeben sich für die obere Bewandung. Für alle untersuchten Wärmestromdichten gilt, daß die maximale Luftgeschwindigkeit senkrecht oberhalb der Zylinderachse im Abstand von ungefähr 9 Zylinderdurchmessern auftritt.

ЕСТЕСТВЕННОКОНВЕКТИВНЫЙ ТЕПЛОПЕРЕНОС МЕЖДУ ОДНОРОДНО НАГРЕВАЕМЫМ ЦИЛИНДРИЧЕСКИМ ЭЛЕМЕНТОМ И ПРЯМОУГОЛЬНОЙ ПОЛОСТЬЮ

Аннотация—С использованием метода спектральных элементов численно исследуется естественноконвективный теплоперенос от однородно нагреваемого горизонтального цилиндра, помещенного в заполненную воздухом большую прямоугольную полость. Стенки полости являются изотермичными, а течение предполагается ламинарным двумерным. Исследуются динамика течения и тепловые характеристики при наложении на цилиндр различных тепловых потоков. Найдено, что среднее число Нуссельта Nu_a изменяется с числом Рэлея Ra_a в соответствии с обобщенной зависимостью вида $Nu_a = C_1(Ra_a)^{C_2}$, где C_1 и C_2—эмпирические постоянные, зависящие от выбранной длины масштаба a. Результирующие постоянные C_2 аналогичны ранее опубликованным постоянным, полученным на основе экспериментальных. Скорости теплопереноса из полости достигают максимума у верхней стенки. Для всех исследуемых тепловых потоков скорость воздуха максимальна на расстоянии, равном около 9 диаметров цилиндра вдоль вертикальной оси над нагретым цилиндром.